Low-Light Image Enhancement through Multi-Scale Local Space Average Color

Oguzhan Ulucan, Diclehan Ulucan, Marc Ebner
University of Greifswald, Institute of Mathematics and Computer Science
17489 Greifswald, Germany
{oguzhan.ulucan, diclehan.ulucan, marc.ebner}@uni-greifswald.de

***Abstract*—Low-light images are common in various fields but often suffer from decreased efficiency due to noise and color degradation. Low-light image enhancement aims to address these issues by producing images similar to those captured under *normal* lighting. Recently, we introduced the first algorithm that addresses both color constancy and color assimilation illusions which is an approach inspired by the human visual system and based on the local space average color method in scale-space. In this paper, we extend our previous work by slightly modifying this strategy for low-light image enhancement. We evaluate our approach against 34 methods across 6 datasets. Experimental results demonstrate that our method effectively illuminates dim scenes, enhances fine details, and eliminates undesired color casts. To the best of our knowledge, this is the first study to integrate color constancy, color illusions, and low-light image enhancement while also demonstrating the impact of the local space average color method in this context. One of the key strengths of our learning-free algorithm is its ability to simultaneously remove color casts and enhance low-light images, producing outputs with vivid colors and eliminating the need for a separate color constancy step.**

***Index Terms*—low-light image enhancement, multiresolution color constancy, illumination estimation.**

I. Introduction

Images captured under poor lighting conditions are often called *low-light images*; however, in practical applications, there are no precise theoretical values defining what constitutes a low-light environment [51]. Low-light images typically suffer from noise, blurriness, color degradation, a narrow gray range, and reduced contrast [37], [51]. Various factors contribute to this decline in image quality, such as lens characteristics, short exposure times, and fast shutter speeds [64]. Low-light image enhancement aims to obtain normal-light images by overcoming these issues.

Enhancing low-light images is crucial for ensuring that they serve as useful data in fields such as video surveillance, object classification, and remote sensing [37]. To address this need, both hardware- and software-based solutions have been proposed. Hardware-based solutions, however, have significant disadvantages: developing robust hardware is laborious because manufacturing low-light circuits and filters requires excellent precision, and high-quality hardware is usually too expensive for everyday use [51]. Furthermore, the lack of an established standard for defining low-light environments means that individual image sensor manufacturers often establish their own criteria [51]. In contrast, software-based solutions typically incur lower costs, and if needed, they can be easily modified. With software, noise can be removed, tone and fine details can be recovered, and the dynamic range and contrast of scenes can be increased which enables both human observers and machine vision systems to extract more information from images [2], [41].

Over the last few decades, numerous image enhancement strategies have been introduced to overcome the challenges posed by low-light scenes [37]. These algorithms can be broadly grouped into two categories: traditional methods [10], [14], [15], [20], [27], [36], [50], [61] and deep learning-based models [5], [6], [23], [24], [28], [30], [34], [49], [53], [56], [60], [63]. Traditional methods typically employ techniques such as histogram equalization, gamma correction, dehazing strategies, image fusion, and the Retinex theory, whereas deep learning-based models utilize approaches like supervised, unsupervised, semi-supervised, and zero-shot learning [37], [64]. Traditional algorithms have strong theoretical foundations and provide simple yet effective solutions, but they may result in color loss and noise generation [51]. On the other hand, machine learning models generally achieve better performance but are heavily dependent on their training sets and have high computational complexity [51].

Recently, we proposed a method that mimics the behavior of the human visual system with respect to two computationally opposing perceptual phenomena: color constancy and color illusions [46]. In our algorithm, we combined the best of two worlds by considering the observations made in computational biology and the experience of white-balancing in computer vision. Our motivation was to address a gap in existing methods. There was no algorithm in computer vision that could be deceived by color illusions while simultaneously performing color constancy, despite the significance of this capability as highlighted in computational biology [8]. Our simple yet effective approach relies on scale-space operations and the fundamentals of local space average color [11], which correspond closely to processes in the human visual system [17], [25], [29]. We modified the local space average color algorithm by applying it across multiple scale-spaces, thereby proposing a *multiresolution color constancy* approach that essentially performs scale-space computations within scale-space computations. In this paper, we extend our previous work by investigating low-light image enhancement from the perspective of our learning-free method. We introduce

slight adjustments to our algorithm without altering its overall framework so that it can perform three different tasks. To the best of our knowledge, this is the first study to address both color constancy and color illusions while also performing low-light image enhancement. Furthermore, it is the first study to analyze the impact of local space average color algorithm in the context of low-light image enhancement. We demonstrate the effectiveness of our algorithm by evaluating our strategy on 6 datasets. Experimental results show that the proposed method can enhance dim images while simultaneously removing color casts using a single pipeline which is an advantage for many vision applications.

II. Computational Color Constancy

We provide a brief introduction to color constancy, which we leverage to enhance scenes captured under low-light conditions. Visual processing begins when photoreceptors in the retina measure the incident light, whereas cameras process visual information when their sensors capture the incident light [44]. Assuming a camera with three distinct sensors, each sensor typically responds to a specific portion of the visible spectrum—namely, short-, middle-, and long-wavelengths. In color constancy, we commonly assume the Lambertian image formation model, where the scene is illuminated by a point light source L. Accordingly, the measured signal I at each spatial location (x, y) can be expressed as:

$$I(x,y) = G(x,y) \int_w R(x,y;\lambda) L(x,y;\lambda) S(\lambda) d\lambda, \quad (1)$$

where R is the reflectance, G is a geometry factor based on the angle between the surface normal and the light source direction, and S represents the camera sensor's spectral sensitivity.

In color constancy, our objective is to determine the illuminant L to obtain a canonical (i.e., white-balanced) image. However, this task is challenging because color constancy is an ill-posed problem; it depends on both the illumination and the sensor characteristics, which are rarely known in real-world applications. To simplify the problem, we assume that there is a spatially uniform light source $\mathbf{L}$ illuminating the scene, the camera sensor responses are narrow-band, and the geometry factor G is uniform throughout the scene [11]. Under these assumptions, any image can be modeled as the Hadamard product of the reflectance R and the illumination $\mathbf{L}$:

$$I(x,y) = R(x,y) \circ \mathbf{L}. \quad (2)$$

Over the decades, numerous color constancy algorithms have been developed [12], [40], [42], [43], [47]. While assuming a single illuminant in a scene can yield visually pleasing images, this assumption is often invalidated in real-world settings due to shadows, multiple light sources, and interreflections [12]. To overcome these issues, some methods assume that the scene is illuminated by spatially varying light, yet the number of these methods is quite limited in comparison to single-illuminant algorithms [1], [3], [11], [45].

III. Proposed Method

Our method is based on key observations of human color processing: *(i)* the information required for illuminant estimation is present in the stimulus at an appropriate scale [38], [39], *(ii)* the human visual system may achieve color constancy by relying on the space average color [4], [11], [25], [29], and *(iii)* global changes caused by the illuminant are primarily carried in the low spatial frequency components; thus, removing blurred content from the input can produce results that align with human perception [9], [38], [39].

A. Revisiting Local Space Average Color

Our approach builds on the local space average color algorithm for the following reasons: *(i)* it has a strong correspondence in the human visual system, *(ii)* it is designed for scenes illuminated with spatially varying lighting conditions, *(iii)* it is independent of training data, and *(iv)* it utilizes only low-level processing to estimate the reflectance of the scene [11].

Local space average color estimates the color of the light sources by using an iterative strategy [11], where convergence may take time. To avoid this high computational cost while achieving comparable results, a convolution operation can be used to calculate the space average color a as follows:

$$a_i(x,y) = k(x,y) \int\int I_i(x,y) g(x-x', y-y') dx' dy', \quad (3)$$

where subscript i represents the color channels of the image, $i \in \{r, g, b\}$, and the scaling factor k is chosen such that

$$k(x,y) \int\int g(x',y') dx' dy' = 1, \quad (4)$$

where g represents the two-dimensional Gaussian kernel defined as $\frac{1}{2\pi\sigma^2} exp(-\frac{x^2+y^2}{2\sigma^2})$. The parameter σ determines the kernel's scale and is typically assigned a value such as $\sigma = \gamma(\max\{h, w\}/2)$, where h and w are the image's height and width, respectively. The choice of γ is crucial to ensure that local averaging covers a sufficiently large region containing a diverse set of objects with varying reflectance properties. This is necessary because the local space average color method assumes that the average color of a scene is gray, a hypothesis that holds only when the scene contains a sufficient variety of colors [11]. For scenes illuminated by a single light source, γ should be chosen larger, while for those illuminated by multiple light sources, a smaller γ is preferable. Unlike our previous work [46], where we accounted for varying illumination, in this study, we assume a dominant single light source. Thus, we utilize a larger γ. In Sec. IV, we compare our initial approach with the modified version adapted for the present study's task.

Finally, the reflectance o of the input scene can be estimated as follows:

$$o(x,y) \approx \frac{I(x,y)}{f a(x,y)}, \quad (5)$$

where f is a scaling factor applied equally to all color channels and is set to 2, assuming a perpendicular orientation between the objects and the capturing device [11].

B. Multiresolution Color Constancy

In our previous work [46], we proposed a *multiresolution color constancy* approach that simultaneously addresses two computationally opposing perceptual phenomena. In this paper, we apply this approach to the task of low-light image enhancement, and this section details our strategy.

Firstly, we determine the number of pyramid levels $n_{\mathcal{L}}$ based on the image resolution as $n_{\mathcal{L}} = \lfloor \log_2(\min(h, w)) \rfloor$. At each pyramid level, we obtain the representations of the input image and compute their pixel-wise light source estimates using the local space average color method (Sec. III-A).

After obtaining the representations of the input scenes with their corresponding local estimates, we perform our multiresolution color constancy strategy. Let l denote a pyramid level, with $l \in \{1, ..., n_{\mathcal{L}}\}$. For the l-th level, we construct a Gaussian pyramid of the local estimates $G\{a_l(x, y)\}$, and a Laplacian pyramid of the input scene $L\{I_l(x, y)\}$, where the number of the scales, $\mathcal{S}$, for both pyramids is determined based on the image resolution, as previously described.

Subsequently, we compute the reflectance at scale s using a similar operation to that in Eqn. 5:

$$\mathcal{P}\{o_l(x, y)\}^s = \frac{\mathcal{L}\{I_l(x, y)\}^s}{\mathcal{G}\{a_l(x, y)\}^s}, \qquad s = 1, 2, \ldots, \mathcal{S}, \quad (6)$$

where we obtain a resulting pyramid $\mathcal{P}\{o_l(x, y)\}$ by repeating this calculation for all scales in $\{1, ..., \mathcal{S}\}$. Then, we collapse the resulting pyramid to obtain an output for the l-th level. We repeat this operation for all levels in $\{1, ..., n_{\mathcal{L}}\}$. This results in a pyramid containing estimated reflectances for all levels in $\{1, ..., n_{\mathcal{L}}\}$. Finally, we collapse this pyramid to obtain a single output reflectance.

C. Contrast Enhancement

Lastly, we enhance the contrast of the output reflectance. Instead of enhancing the luminance via CLAHE [65] as in our previous work [46], in this study, we perform percentile-based contrast stretching (this design choice is detailed in Sec. IV).

We begin by applying the gray-world algorithm [4] to the input image I. Afterwards, we convert the image from RGB to the CIELAB color space (we utilize $D65$ as white point and using other white points has ignorable effects on the results) and extract the luminance component L^*. To enhance the contrast of L^* while minimizing the influence of outliers, we employ a percentile-based contrast stretching approach. Specifically, the 0.5th and 99.5th percentiles of the intensity distribution are computed, with values below the 0.5th percentile clipped to the minimum, and those above the 99.5th percentile clipped to the maximum. Then, we use the same percentiles to enhance the L^* channel of the output reflectance, ensuring consistency in contrast adjustments.

Afterwards, we linearly combine the enhanced L^* from the input image with the enhanced L^* channel of the output reflectance. Finally, we recombine the resulting luminance component with the a^* and b^* chromaticity channels of the output reflectance, and convert the modified image back into the RGB color space to produce our final output.

IV. Experiments and Discussion

We provide a comprehensive comparison with 34 algorithms across 6 datasets. We evaluate our algorithm on the LOL-v1 and LOL-v2 datasets [53], [60], which include ground truth images, and on the MEF [31], DICM [26], LIME [19], and VV [48] datasets, which do not contain ground truths. For the former, we benchmark our algorithm using the peak signal-to-noise ratio (PSNR) and the structural similarity index (SSIM) [52], while for the latter, we use the natural image quality evaluator (NIQE) [33]. We report the results based on either the codes provided by the authors or other works that are considered comprehensive and up-to-date [5], [21], [22].

As shown in Table I and Table II, our algorithm achieves competitive performance on all datasets, ranking among the top 3 methods. Our learning-free algorithm relying entirely on low-level processing, outperforms traditional algorithms and competes with state-of-the-art models by effectively recovering details in low-light images. Furthermore, the proposed method, explicitly designed to address color constancy and color illusions [46], successfully restores fine details in low-light conditions. Notably, when low-light scenes contain color tints caused by illumination effects, other algorithms often introduce noise and undesirable color casts in their outputs, as illustrated in the first row of Fig. 1. In contrast, our multiresolution color constancy method largely avoids these issues, producing low-light enhanced white-balanced outputs. It is worth noting that correcting also the color casts in the

TABLE I
COMPARISON ON DATASETS WITH GROUND TRUTH. LEARNING-BASED METHODS ARE MARKED WITH *. TOP FIVE RESULTS ARE COLOR-CODED: BEST, SECOND, THIRD, FORTH, FIFTH.

	LOL-v1		LOL-v2			LOL-v1		LOL-v2	
Algorithm	PSNR↑	SSIM↑	PSNR↑	SSIM↑	Algorithm	PSNR↑	SSIM↑	PSNR↑	SSIM↑
Dong *et al.* [10]	16.72	0.58	17.26	0.52	Wang *et al.** [49]	14.38	0.44	13.27	0.45
Wang *et al.* [50]	16.97	0.59	17.34	0.51	Moran *et al.** [34]	15.28	0.47	14.10	0.48
Lee *et al.* [27]	11.91	0.41	15.37	0.47	Chen *et al.** [7]	16.27	0.50	19.80	0.81
Petro *et al.* [36]	15.37	0.51	13.58	0.40	Li *et al.** [28]	21.46	0.80	17.80	0.79
Fu *et al.* [15]	11.86	0.50	17.34	0.68	Xu *et al.** [56]	18.27	0.66	16.85	0.67
Ying *et al.* [61]	13.86	0.58	17.85	0.65	Jiang *et al.** [22]	20.45	0.80	-	-
Fu *et al.* [14]	18.79	0.64	18.73	0.55	Kosugi and Yamasaki* [24]	15.23	0.45	14.05	0.45
Guo *et al.* [20]	16.76	0.56	15.24	0.47	Jiang *et al.** [23]	17.48	0.65	18.23	0.61
Ma *et al.** [32]	14.78	0.65	20.28	0.75	Yang *et al.** [59]	19.86	0.83	20.13	0.83
Yang *et al.** [58]	19.74	0.74	-	-	Liu *et al.** [30]	18.23	0.72	18.37	0.72
Wei *et al.** [53]	16.77	0.56	15.47	0.56	Yang *et al.** [60]	17.20	0.64	20.06	0.81
Wei *et al.** [54]	-	-	20.79	0.79	Nguyen *et al.** [35]	23.97	0.84	-	-
Chen *et al.** [6]	14.35	0.43	13.24	0.44	Cai *et al.** [5]	25.16	0.84	22.80	0.84
Fei *et al.** [13]	15.90	0.54	-	-	Fu *et al.** [16]	19.51	0.73	-	-
Wu *et al.** [55]	21.33	0.84	21.16	0.84	Initial Version [46]	20.46	0.72	19.66	0.70
Zhang *et al.** [63]	20.87	0.80	14.47	0.64	**Proposed**	22.28	0.80	21.58	0.81

TABLE II
COMPARISON ON DATASETS WITHOUT GROUND TRUTH. TOP THREE RESULTS ARE COLOR-CODED: BEST, SECOND, THIRD. LOWER NIQE INDICATES BETTER RESULTS.

Algorithm	MEF	DICM	LIME	VV
Xu *et al.** [57]	6.44	6.12	5.93	11.50
Zhang *et al.** [62]	4.55	3.89	4.90	3.82
Hou *et al.** [21]	3.40	3.28	4.32	2.60
Guo *et al.** [18]	4.93	4.58	5.82	4.81
Wei *et al.** [53]	4.93	4.33	5.75	4.32
Proposed	4.24	4.12	4.62	3.80

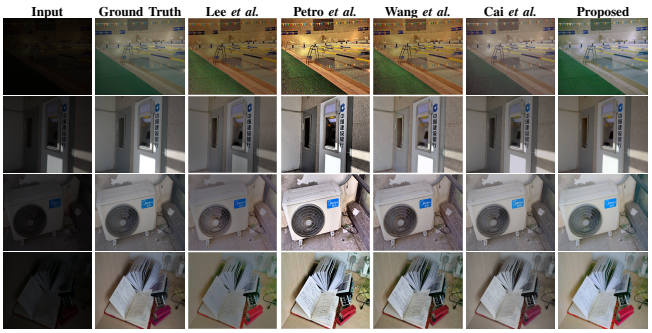

Fig. 1. Visual comparison on random examples.

scenes can influence the statistical results. Specifically, ground truths containing color shifts that our method removes, may lead to discrepancies in evaluations, even though our approach successfully enhances the images. We do not white-balance the ground truths, as doing so would compromise fairness, especially since other low-light image enhancement methods evaluate their results against the unaltered ground truths.

We also analyze the effects of using different contrast enhancement methods on our algorithm's performance (Table III). On both datasets, percentile-based contrast stretching yields the best results compared to histogram equalization and CLAHE. Thus, we employ this approach in our algorithm.

As a final note, we discuss the advantages and limitations of our method. Compared to traditional algorithms, our approach produces outputs with vivid colors while exhibiting reduced noise and color shifts (Fig.1). Unlike many traditional methods, our approach does not rely on solving optimization problems or requiring heavily tuned parameters [51]. Additionally, unlike fusion-based methods, which need multiple inputs with varying exposure settings to correct low-light conditions, our method operates on a single image. This is a significant advantage in real-world applications, where capturing multiple images with appropriate settings can be challenging. Another key strength of our method is its ability to simultaneously enhance low-light images and correct color casts, eliminating the need for a separate color constancy step. This integrated ability is valuable for many computer vision tasks such as object detection, where low-light conditions and color distortions can affect accuracy. By addressing both challenges in one step, our method ensures brighter, color-accurate images while simplifying the pipeline. Compared to learning-based algorithms, our method offers lower computational complexity and is independent of training data. However, it remains more prone to noise than state-of-the-art learning-based models.

TABLE III
STATISTICAL COMPARISON OF DIFFERENT VERSIONS OF OUR METHOD.

	LOL-v1		LOL-v2	
Approach	PSNR↑	SSIM↑	PSNR↑	SSIM↑
w/ Histogram Equalization	17.38	0.66	18.49	0.68
w/ CLAHE	17.82	0.72	19.15	0.75
w/ Percentile-based Contrast Stretching	**22.28**	**0.80**	**21.58**	**0.81**

V. CONCLUSION

Low-light image enhancement plays a key role in real-world applications. In this study, we investigate this field from the perspective of our recently introduced algorithm that performs color constancy and mimics our behavior on color assimilation illusions. The proposed approach combines the local space average color method with our multiresolution color constancy strategy which uses scale-space within scale-space computations. We demonstrate that our learning-free method achieves competitive results across 6 datasets, while outperforming the traditional methods, and several state-of-the-art learning-based strategies. To the best of our knowledge, this is the first approach that is able to perform color constancy and reproduce our sensation on color illusions, while also carrying out low-light image enhancement, simultaneously. Our learning-free method's key advantage lies in its ability to enhance and white-balance low-light images without requiring a separate color constancy step, which makes it particularly suited for various imaging applications.

REFERENCES

[1] M. Afifi, M. A. Brubaker, and M. S. Brown, "Auto white-balance correction for mixed-illuminant scenes," in *IEEE/CVF Winter Conf. Appl. Comput. Vision*, 2022, pp. 1210–1219.
[2] M. Afifi, Z. Hu, and L. Liang, "Optimizing illuminant estimation in dual-exposure hdr imaging," in *European Conf. Comput. Vision*. Springer, 2024, pp. 202–219.
[3] S. Bianco, C. Cusano, and R. Schettini, "Single and multiple illuminant estimation using convolutional neural networks," *IEEE Trans. Image Process.*, vol. 26, no. 9, pp. 4347–4362, 2017.
[4] G. Buchsbaum, "A spatial processor model for object colour perception," *J. Franklin Inst.*, vol. 310, pp. 1–26, 1980.
[5] Y. Cai, H. Bian, J. Lin, H. Wang, R. Timofte, and Y. Zhang, "Retinexformer: One-stage retinex-based transformer for low-light image enhancement," in *IEEE/CVF Int. Conf. Comput. Vision*, 2023, pp. 12 504–12 513.
[6] C. Chen, Q. Chen, M. N. Do, and V. Koltun, "Seeing motion in the dark," in *IEEE/CVF Int. Conf. Comput. Vision*, 2019, pp. 3185–3194.
[7] H. Chen, Y. Wang, T. Guo, C. Xu, Y. Deng, Z. Liu, S. Ma, C. Xu, C. Xu, and W. Gao, "Pre-trained image processing transformer," in *IEEE/CVF Conf. Comput. Vision Pattern Recognit.*, 2021, pp. 12 299–12 310.
[8] D. Corney and R. B. Lotto, "What are lightness illusions and why do we see them?" *PLoS Comput. Biol.*, vol. 3, no. 9, p. e180, 2007.
[9] E. L. Dixon and A. G. Shapiro, "Spatial filtering, color constancy, and the color-changing dress," *J. Vision*, vol. 17, no. 3, pp. 7–7, 2017.
[10] X. Dong, G. Wang, Y. Pang, W. Li, J. Wen, W. Meng, and Y. Lu, "Fast efficient algorithm for enhancement of low lighting video," in *IEEE Int. Conf. Multimedia Expo*. IEEE Computer Society, 2011, pp. 1–6.
[11] M. Ebner, "Color constancy based on local space average color," *Mach. Vision Appl.*, vol. 20, no. 5, pp. 283–301, 2009.
[12] E. Ershov, V. Tesalin, I. Ermakov, and M. S. Brown, "Physically-plausible illumination distribution estimation," in *IEEE/CVF Int. Conf. Comput. Vision*, 2023, pp. 12 928–12 936.
[13] Z. Fei, B.and Lyu, L. Pan, J. Zhang, W. Yang, T. Luo, B. Zhang, and B. Dai, "Generative diffusion prior for unified image restoration and enhancement," in *IEEE/CVF Conf. Comput. Vision Pattern Recognit.*, 2023, pp. 9935–9946.
[14] X. Fu, D. Zeng, Y. Huang, Y. Liao, X. Ding, and J. Paisley, "A fusion-based enhancing method for weakly illuminated images," *Signal Process.*, vol. 129, pp. 82–96, 2016.
[15] X. Fu, D. Zeng, Y. Huang, X.-P. Zhang, and X. Ding, "A weighted variational model for simultaneous reflectance and illumination estimation," in *IEEE Conf. Comput. Vision Pattern Recognit.*, 2016, pp. 2782–2790.
[16] Z. Fu, Y. Yang, X. Tu, Y. Huang, X. Ding, and K.-K. Ma, "Learning a simple low-light image enhancer from paired low-light instances," in *IEEE/CVF Conf. Comput. Vision Pattern Recognit.*, 2023, pp. 22 252–22 261.

[17] K. R. Gegenfurtner, "Cortical mechanisms of colour vision," *Nature Reviews Neuroscience*, vol. 4, no. 7, pp. 563–572, 2003.

[18] C. Guo, C. Li, J. Guo, C. C. Loy, J. Hou, S. Kwong, and R. Cong, "Zero-reference deep curve estimation for low-light image enhancement," in *IEEE/CVF Conf. Comput. Vision Pattern Recognit.*, 2020, pp. 1780–1789.

[19] X. Guo, "Lime: A method for low-light image enhancement," in *ACM Int. Conf. Multimedia*, 2016, pp. 87–91.

[20] X. Guo, Y. Li, and H. Ling, "Lime: Low-light image enhancement via illumination map estimation," *IEEE Trans. Image Process.*, vol. 26, no. 2, pp. 982–993, 2016.

[21] J. Hou, Z. Zhu, J. Hou, H. Liu, H. Zeng, and H. Yuan, "Global structure-aware diffusion process for low-light image enhancement," *Advances Neural Inf. Process. Syst.*, vol. 36, 2024.

[22] H. Jiang, A. Luo, X. Liu, S. Han, and S. Liu, "Lightendiffusion: Unsupervised low-light image enhancement with latent-retinex diffusion models," in *European Conf. Comput. Vision*, 2025, pp. 161–179.

[23] Y. Jiang, X. Gong, D. Liu, Y. Cheng, C. Fang, X. Shen, J. Yang, P. Zhou, and Z. Wang, "Enlightengan: Deep light enhancement without paired supervision," *IEEE Trans. Image Process.*, vol. 30, pp. 2340–2349, 2021.

[24] S. Kosugi and T. Yamasaki, "Unpaired image enhancement featuring reinforcement-learning-controlled image editing software," in *AAAI Conf Artif. Intell.*, 2020, pp. 11 296–11 303.

[25] E. H. Land, "The retinex theory of colour vision," *Proc. Roy. Institution Gr. Britain*, vol. 47, pp. 23–58, 1974.

[26] C. Lee, C. Lee, and C.-S. Kim, "Contrast enhancement based on layered difference representation of 2d histograms," *IEEE Trans. Image Process.*, vol. 22, no. 12, pp. 5372–5384, 2013.

[27] C.-H. Lee, J.-L. Shih, C.-C. Lien, and C.-C. Han, "Adaptive multiscale retinex for image contrast enhancement," in *Int. Conf. Signal Image Technol. Internet-Based Syst.* IEEE, 2013, pp. 43–50.

[28] J. Li, J. Li, F. Fang, F. Li, and G. Zhang, "Luminance-aware pyramid network for low-light image enhancement," *IEEE Trans. Multimedia*, vol. 23, pp. 3153–3165, 2020.

[29] K. J. Linnell and D. H. Foster, "Space-average scene colour used to extract illuminant information," *John Dalton's Colour Vision Legacy*, pp. 501–509, 1997.

[30] R. Liu, L. Ma, J. Zhang, X. Fan, and Z. Luo, "Retinex-inspired unrolling with cooperative prior architecture search for low-light image enhancement," in *IEEE/CVF Conf. Comput. Vision Pattern Recognit.*, 2021, pp. 10 561–10 570.

[31] K. Ma, K. Zeng, and Z. Wang, "Perceptual quality assessment for multi-exposure image fusion," *IEEE Trans. Image Process.*, vol. 24, no. 11, pp. 3345–3356, 2015.

[32] L. Ma, T. Ma, R. Liu, X. Fan, and Z. Luo, "Toward fast, flexible, and robust low-light image enhancement," in *IEEE/CVF Conf. Comput. Vision Pattern Recognit.*, 2022, pp. 5637–5646.

[33] A. Mittal, R. Soundararajan, and A. C. Bovik, "Making a "completely blind" image quality analyzer," *IEEE Signal Process. Letters*, vol. 20, no. 3, pp. 209–212, 2012.

[34] S. Moran, P. Marza, S. McDonagh, S. Parisot, and G. Slabaugh, "Deeplpf: Deep local parametric filters for image enhancement," in *IEEE/CVF Conf. Comput. Vision Pattern Recognit.*, 2020, pp. 12 826–12 835.

[35] C. M. Nguyen, E. R. Chan, A. W. Bergman, and G. Wetzstein, "Diffusion in the dark: A diffusion model for low-light text recognition," in *IEEE/CVF Winter Conf. Appl. Comput. Vision*, 2024, pp. 4146–4157.

[36] A. B. Petro, C. Sbert, and J.-M. Morel, "Multiscale retinex," *Image Process. on line*, pp. 71–88, 2014.

[37] M. T. Rasheed, D. Shi, and H. Khan, "A comprehensive experiment-based review of low-light image enhancement methods and benchmarking low-light image quality assessment," *Signal Process.*, vol. 204, p. 108821, 2023.

[38] A. Shapiro, L. Hedjar, E. Dixon, and A. Kitaoka, "Kitaoka's tomato: two simple explanations based on information in the stimulus," *i-Perception*, vol. 9, no. 1, p. 2041669517749601, 2018.

[39] A. Shapiro and Z.-L. Lu, "Relative brightness in natural images can be accounted for by removing blurry content," *Psychological Sci.*, vol. 22, no. 11, pp. 1452–1459, 2011.

[40] B. Simone and R. Schettini, "Color constancy using faces," in *IEEE Conf. Comput. Vis. Pattern Recog.*, 2012, pp. 65–72.

[41] O. Ulucan, D. Karakaya, and M. Turkan, "Multi-exposure image fusion based on linear embeddings and watershed masking," *Signal Process.*, vol. 178, p. 107791, 2021.

[42] O. Ulucan, D. Ulucan, and M. Ebner, "BIO-CC: Biologically inspired color constancy," in *Brit. Mach. Vision Conf.*, 2022.

[43] O. Ulucan, D. Ulucan, and M. Ebner, "Color constancy beyond standard illuminants," in *IEEE Int. Conf. Image Process.*, 2022, pp. 2826–2830.

[44] O. Ulucan, D. Ulucan, and M. Ebner, "Block-based color constancy: The deviation of salient pixels," in *IEEE Int. Conf. Acoust. Speech Signal Process.*, 2023, pp. 1–5.

[45] O. Ulucan, D. Ulucan, and M. Ebner, "Multi-scale color constancy based on salient varying local spatial statistics," *The Vis. Comput.*, pp. 1–17, 2023.

[46] O. Ulucan, D. Ulucan, and M. Ebner, "A computational model for color assimilation illusions and color constancy," in *Asian Conf. Comput. Vision*, 2024, pp. 630–647.

[47] O. Ulucan, D. Ulucan, and M. Ebner, "Revisiting color constancy using cnns: Including recent observations," in *Int. Workshop Comput. Color Imag.* Springer, 2024, pp. 261–273.

[48] V. Vonikakis, R. Kouskouridas, and A. Gasteratos, "On the evaluation of illumination compensation algorithms," *Multimedia Tools Appl.*, vol. 77, pp. 9211–9231, 2018.

[49] R. Wang, Q. Zhang, C.-W. Fu, X. Shen, W.-S. Zheng, and J. Jia, "Underexposed photo enhancement using deep illumination estimation," in *IEEE/CVF Conf. Comput. Vision Pattern Recognit.*, 2019, pp. 6849–6857.

[50] S. Wang, J. Zheng, H.-M. Hu, and B. Li, "Naturalness preserved enhancement algorithm for non-uniform illumination images," *IEEE Trans. Image Process.*, vol. 22, no. 9, pp. 3538–3548, 2013.

[51] W. Wang, X. Wu, X. Yuan, and Z. Gao, "An experiment-based review of low-light image enhancement methods," *IEEE Access*, vol. 8, pp. 87 884–87 917, 2020.

[52] Z. Wang, A. C. Bovik, H. R. Sheikh, and E. P. Simoncelli, "Image quality assessment: from error visibility to structural similarity," *IEEE Trans. Image Process.*, vol. 13, no. 4, pp. 600–612, 2004.

[53] C. Wei, W. Wang, W. Yang, and J. Liu, "Deep retinex decomposition for low-light enhancement," in *Brit. Mach. Vision Conf.*, 2018, pp. –.

[54] X. Wei, X. Lin, and Y. Li, "Da-drn: A degradation-aware deep retinex network for low-light image enhancement," *Digit. Signal Process.*, vol. 144, p. 104256, 2024.

[55] W. Wu, J. Weng, P. Zhang, X. Wang, W. Yang, and J. Jiang, "Uretinex-net: Retinex-based deep unfolding network for low-light image enhancement," in *IEEE/CVF Conf. Comput. Vision Pattern Recognit.*, 2022, pp. 5901–5910.

[56] K. Xu, X. Yang, B. Yin, and R. W. Lau, "Learning to restore low-light images via decomposition-and-enhancement," in *IEEE/CVF Conf. Comput. Vision Pattern Recognit.*, 2020, pp. 2281–2290.

[57] X. Xu, R. Wang, C.-W. Fu, and J. Jia, "Snr-aware low-light image enhancement," in *IEEE/CVF Conf. Comput. Vision Pattern Recognit.*, 2022, pp. 17 714–17 724.

[58] S. Yang, M. Ding, Y. Wu, Z. Li, and J. Zhang, "Implicit neural representation for cooperative low-light image enhancement," in *IEEE/CVF Int. Conf. Comput. Vision*, 2023, pp. 12 918–12 927.

[59] W. Yang, S. Wang, Y. Fang, Y. Wang, and J. Liu, "From fidelity to perceptual quality: A semi-supervised approach for low-light image enhancement," in *IEEE/CVF Conf. Comput. Vision Pattern Recognit.*, 2020, pp. 3063–3072.

[60] W. Yang, W. Wang, H. Huang, S. Wang, and J. Liu, "Sparse gradient regularized deep retinex network for robust low-light image enhancement," *IEEE Trans. Image Process.*, vol. 30, pp. 2072–2086, 2021.

[61] Z. Ying, G. Li, and W. Gao, "A bio-inspired multi-exposure fusion framework for low-light image enhancement," *arXiv preprint arXiv:1711.00591*, 2017.

[62] Y. Zhang, X. Guo, J. Ma, W. Liu, and J. Zhang, "Beyond brightening low-light images," *Int. J. Comput. Vision*, vol. 129, pp. 1013–1037, 2021.

[63] Y. Zhang, J. Zhang, and X. Guo, "Kindling the darkness: A practical low-light image enhancer," in *ACM Int. Conf. Multimedia*, 2019, pp. 1632–1640.

[64] S. Zheng, Y. Ma, J. Pan, C. Lu, and G. Gupta, "Low-light image and video enhancement: A comprehensive survey and beyond," *arXiv preprint arXiv:2212.10772*, 2022.

[65] K. Zuiderveld, "Contrast limited adaptive histogram equalization," *Graph. Gems*, pp. 474–485, 1994.